Rotor Dynamic Analysis in Power Lost Condition for Maglev High-speed Fluid Machinery

Chao-Yun Chen [a] , Chung-Che Liu[a], Aindri Yuliane [b], and Yean-Der Kuan [b]

[a] Green Energy and Environment Research Laboratories, Industrial Technology Research Institute, Hsinchu, 31040, Taiwan, Email: cychen1022@itri.org.tw

[b] Department of Refrigeration, Air Conditioning and Energy Engineering, National Chin-Yi University of Technology, Taichung, 41170, Taiwan

***Abstract*—The advantages offered by active magnetic bearings make that bearing widely used in high-speed Fluid Machinery, the applications that use active magnetic bearing must be equipped with touchdown (auxiliary) bearing system to prevent the damages of impellers and motor in case of a system failure. When the drop event occurs, active magnetic bearing cannot support the rotor stably, touchdown bearings will be a backup for active magnetic bearings to support the rotor during drop down event. Therefore, the properly designed touchdown bearing system is necessary to protect the active magnetic bearings assembly and other critical machine components from direct contact with the rotor during in a loss of AMB power events. This study has based on the un-lubricated Hertzian contact model to analyze the rotor drop dynamics, and the Finite Element method is used to create the flexible rotor model. Finally, the simulation results of this study will show the rotor orbit, rotor response and contact force under rotor drop events by using MATLAB software.**

I. INTRODUCTION

The advance development in technology brings an impact to the application of active magnetic bearing which is has been used more widely in the high-speed Fluid Machinery. The advantages of magnetic bearings are no physical contact between rotating and stationary, minimal friction and wear, and do not need lubrication system etc. Auxiliary bearing is the important components that must be equipped in the applications, the features of auxiliary bearing is to prevent the damages of impellers and motor when magnetic bearing failed to operate. Some researchers called auxiliary bearing as catcher bearing, retainer bearing or auxiliary bearing. In this study the auxiliary bearing called as touchdown bearings.

Touchdown bearings will be used when the drop event occurs. In that condition, active magnetic bearing cannot support the rotor stably and touchdown bearings will be a backup for active magnetic bearings to support the rotor during drop down event. Therefore, without appropriate knowledge of retainer bearings, there is a chance that an AMB supported rotor system will be fatal in a dropdown situation. Sun et al. presented the detailed ball bearing model for magnetic suspension auxiliary service [1]. The results reveal that friction coefficient, support damping and side loads are critical parameters to satisfy catcher bearing design objective and prevent backward (super whirl). Cao et al. [2] presented the detailed formulation of a nonlinear transient analysis for rotor drop event. In the dropdown situation, when the rotor drops from the magnetic bearings to the touchdown bearings, the design parameters of the touchdown bearings have a significant influence on the behavior of the rotor. Dynamic simulation of the rotor can be used to simulate the response and behavior of the rotor. Many researchers studied about the design parameter for touchdown bearings to know the effect to the response and behavior of the rotor. Various design parameters of touchdown bearings are studied using simulation model such as the friction coefficient, mass of unbalance, stiffness and damping support coefficient [3-4].

The failure of AMBs generates a highly non-linear behavior or interaction of the rotor with touchdown bearings [5-8]. Based on that statement, it needs identification to simulate the interaction of the rotor and touchdown bearing in order to clarify uncertainty encountered during the drop event (AMB failure). The uncertainty encountered during AMB failure pertains to the rotor behavior. Therefore, this study presents the dynamic simulation of the rotor to simulate the response and behavior of the rotor during the drop event. The rotor behavior can be seen by the rotor response or rotor motion, so that the rotor need to model in the simulation. Some researchers were modelling the rotor as rigid rotor in their simulation [9-10]. However, in this study the rotor modelled as flexible rotor and solved by finite element method using MATLAB software. Finally, the effect of rotor speed and the design of touchdown bearing (with or without damping and stiffness support) will be examined to see and analyze the rotor behavior based on the rotor orbit, rotor response and contact force.

II. ROTOR FINITE ELEMENT MODEL

In this study, the rotor finite element model is solved by using MATLAB software. Finite element modelling methods have been largely used for flexible shaft in Active Magnetic Bearing modelling. Finite element method is obtained by dividing geometry into a number of elements depending on geometry shape and these elements are connected to each other with nodes. This table below shows the detail rotor finite element model.

TABLE I. ROTOR FINITE ELEMENT MODEL

Detail Element Data	
Number of elements	72
Number of nodes	73
Number degrees of freedom	2
Total number degrees of freedom	146
Rotor length	
Magnetic bearing nodes	22 & 61
Touchdown bearing nodes	13 & 70

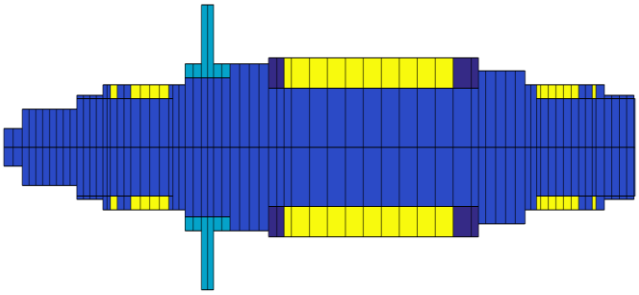

Figure 1. The finite element model of the flexible rotor with beam elemnts

III. MATHEMATICAL MODEL OF ROTOR DROP

Active Magnetic Bearing system (AMB system) has two different motion equations; motion before drop event and motion after drop event. Motion before drop event means that the rotor is supported by active magnetic bearing (AMB). However, when a loss of AMB power is occurred in the system, the rotor is dropped onto touchdown bearing because active magnetic bearing can't support the rotor stably. That condition called as motion after drop event. Fig. 2 illustrates the rotor model, with K_c is contact stiffness that occurred when there is a contact between shaft and inner race bearing. K_b and C_b are the stiffness and damping of auxiliary bearing, then K_s and C_s are the stiffness and damping support which are located outside of the outer races if they exist.

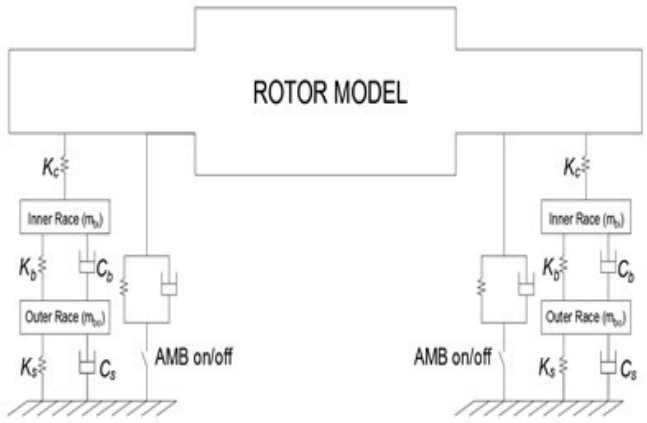

Figure 2. Rotor model

Finally, considering the external forces acting on the rotor that included contact force(F_c), touchdown bearing force(F_b), unbalance force (F_u) and gravity force(F_g), the general rotor dynamic equation of motion after drop event is expressed as:

$$\mathrm{M}\ddot{q} + (\mathrm{C} + \omega\mathrm{G})\dot{q} + \mathrm{K}q = F_c + F_b + F_u + F_g \quad (1)$$

where M is the mass matrix, C is the damping matrix, G is the gyroscopic matrix, K is the stiffness matrix, ω is the rotation speed, and q presents the displacement vector.

A. Contact Force Model

When the rotor dropped onto touchdown bearing there will be a contact between the shaft and touchdown bearing (inner race) because the changing of the clearance. It called as touchdown bearing gap. The air gap for touchdown bearing is typically half of the air gap of AMB system. Therefore, when the contact is occurred, it generates the contact force. Contact force model that used in this study refers to Liu et.al [11].

$$F_{cx1,2} = F_{n1,2}\cos\psi_{1,2} - F_{t1,2}\sin\psi_{1,2} \quad (2)$$

$$F_{cy1,2} = F_{n1,2}\sin\psi_{1,2} + F_{t1,2}\cos\psi_{1,2} \quad (3)$$

F_n is the normal force and F_t is the friction force which acts perpendicular to the normal force as shown in Fig. 3.

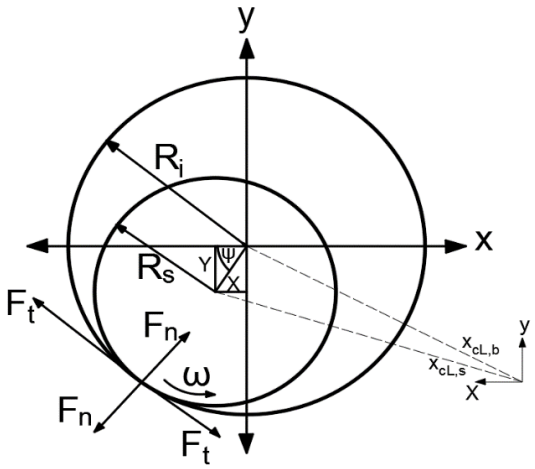

Figure 3. Shaft – inner race contact model

Besides that, from Fig. 3 the contact angle between shaft and inner race bearing can be obtained as follows:

$$\psi_{1,2} = \tan^{-1}\left(\frac{Y_{1,2}}{X_{1,2}}\right) \quad (4)$$

Subscripts 1 and 2 represent for front and rear touchdown bearings. Then, normal contact force (F_n) and friction force (F_t) obtained by:

$$\|F_{n1,2}\| = \begin{cases} \frac{\pi}{2}\delta_{r1,2}EL\sqrt{\frac{\delta_{r1,2}}{2\left((R_i-R_s)+\delta_{r1,2}\right)}} & \delta_{r1,2} > 0 \\ 0 & \delta_{r1,2} \le 0 \end{cases} \quad (5)$$

Where δ_r is the shaft / race deflection, which is given by:

$$\delta_{r1,2} = \sqrt{{X_{1,2}}^2 + {Y_{1,2}}^2} - (R_i - R_s) \quad (6)$$

Here X and Y are the shaft center location, whereas R_i and R_s are radius of inner race and shaft. E is the shaft Young's Modulus and L is the contact length.

If the contact occurs, the normal force line of action will be collinear with $x_{b,s}$. The direction of normal force acting on the rotor will be opposite that of $x_{b,s}$. A unit vector pointing in the direction of the normal force exerted on the rotor $\hat{c}_n$ can be obtained by:

$$\hat{c}_n = -\frac{x_{cL,s} - x_{cL,b}}{\left\| x_{cL,s} - x_{cL,b} \right\|} \quad (7)$$

Considering the value of $\hat{c}_n$, the normal force is completely determined:

$$F_{n1,2} = \left\| F_{n1,2} \right\| . \hat{c}_n \quad (8)$$

When the rotor and touchdown bearing are in contact, the speed of touchdown bearings will increase up to shaft speed, while the speed of shaft will decelerate. Those conditions will be affected to the velocity of both surfaces (inner race surface velocity and shaft surface velocity) which can determine the friction coefficient (μ_r) to calculate friction force as follows:

$$\mu_r = \begin{cases} \mu_d, & v_s > v_i \quad (kinetic) \\ \mu_s, & v_s = v_i \quad (static) \\ -\mu_d, & v_s < v_i \quad (kinetic) \end{cases}$$

where the inner race (v_i) and shaft velocity (v_s) can be obtained by:

$$v_i = (\omega_i \, x \, R_i) \quad (9)$$

$$v_s = (\omega_s \, x \, R_s) \quad (10)$$

Considering the unit vector in the direction of frictional force, finally the equation of friction force ($F_{t1,2}$) is expressed as:

$$F_{t1,2} = \mu_r . \left\| F_{n1,2} \right\| . \hat{c}_t \quad (11)$$

$$\hat{c}_t = -\frac{v_i - v_s}{\| v_i - v_s \|} \quad (12)$$

B. Touchdown Bearing Force

The system that used active magnetic bearing must be equipped by touchdown bearings as auxiliary bearings. There are two kinds of touchdown bearing; ball bearings and sleeve bearings. However, ball bearings are commonly used than sleeve bearings. If compared with sleeve bearings, ball bearings have some advantages. As the rolling elements, ball bearings have low friction, compact size and unlubricated operation.

A ball bearing consists of a number of moving parts. For each ball, there are normal compressive force, centrifugal force and ball gyroscopic moments. However, in this study the touchdown bearings are modelled by neglecting the ball centrifugal force and gyroscopic moment, some researchers also neglected those force to reduce simulation time. Neglecting both forces, the direct method uses the following equations:

$$Q_j = k_{rb} \delta_j^{\frac{3}{2}} \quad (13)$$

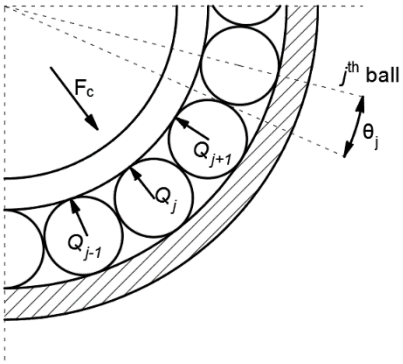

Figure 4. Contact force affecting inner race bearing

The total deformation (δ_j) and the total stiffness (k_{rb}) of the inner and outer ball-raceway can be determined by using Hertzian contact stiffness [12]. k_i and k_o are the inner and outer race stiffness of ball bearings, those values are depended by the geometric and material properties of ball and raceway which can be determined as follows:

$$k_{rb} = \left[\frac{1}{\left(\frac{1}{k_i}\right)^{2/3} + \left(\frac{1}{k_o}\right)^{2/3}} \right]^{3/2} \quad (14)$$

$$k_{i,o} = \frac{2^{2.5}}{3\left(\frac{(1 - {v_{i,o}}^2)}{E_{i,o}} + \frac{(1 - {v_b}^2)}{E_b}\right)(\delta^*)^{1.5}\sqrt{\sum \rho_{i,o}}} \quad (15)$$

where

$v_{i,o}$ = Poisson ratio of inner and outer raceway

v_b = Poisson ratio of bearing's ball

$E_{i,o}$ = Inner and outer race Young's modulus

E_b = Bearing's ball Young's modulus

$\sum \rho_{i,o}$ = Inner and outer race curvature sum

The parameter (δ^*) is function of curvature difference $F_{(\rho)}$ and the relationship between both values are given in Table 6-based on Harris's Handbook [12].

$$F_{(\rho)\mathrm{i}} = \frac{{}^{1}/_{f_i} + {}^{2\gamma}/_{1-\gamma}}{4 - {}^{1}/_{f_i} + {}^{2\gamma}/_{1-\gamma}};\ F_{(\rho)\mathrm{o}} = \frac{{}^{1}/_{f_o} - {}^{2\gamma}/_{1+\gamma}}{4 - {}^{1}/_{f_o} - {}^{2\gamma}/_{1+\gamma}}; \quad (16)$$

$$\sum \rho_i = \frac{1}{D_b}\left(4 - \frac{1}{f_i} + \frac{2\gamma}{1-\gamma}\right);\ \sum \rho_i = \frac{1}{D_b}\left(4 - \frac{1}{f_o} - \frac{2\gamma}{1+\gamma}\right) \quad (17)$$

Referred to Antti [13], finally the resultant touchdown bearing forces applied to the shaft in X and Y direction as follows:

$$F_{bx} = -\sum_{j=1}^{z} Q_j \cos\theta_j \quad (18)$$

$$F_{by} = -\sum_{j=1}^{z} Q_j \sin\theta_j \quad (19)$$

IV. Simulation Results

This section presents the simulation results of rotor drop event. The rotor drop equations based on Eq. 1 is solved by using Finite Element Method. Fig. 5 describes the flowchart of the simulation process. This simulation results will show the rotor orbit, rotor response and contact force with different rotor speed using the original design based on Table 3. Beside that this study will also make an improvement to the original design by adding the damping support and stiffness support.

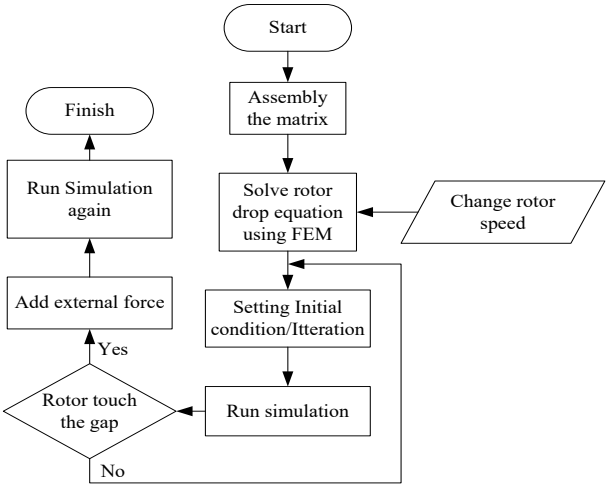

Figure 5. Flowchart rotor drop simulation

TABLE II. Rotor specifications

Specifications	Value
Mass of rotor (m)	32 kg
Rotor speed	18000 RPM
Shaft radius (R_s)	29.9x10^{-3} m
Rotor eccentricity (u)	1.25x10^{-6} m
Air gap between rotor and touchdown bearing	1x10^{-4} m
Rotor moment of inertia (I_r)	0.795 kg.m^2

TABLE III. Touchdown bearing specifications

Specifications	Value
Inner & outer radius (R_I & R_O)	0.03 m & 0.0425 m
Number of balls (Z)	27
Ball diameter (D_b)	7.938 x10^{-3} m
Touchdown bearing stiffness (K_b)	1.32x10^8 N/m
Raceway Young's modulus ($E_{i,o}$)	208 GPa
Raceway Poisson Ratio ($v_{i,o}$)	0.3
Ball Young's modulus (E_b)	300~320 GPa
Ball poisson ratio (v_b)	0.26
Damping support (C_s)	-
Stiffness support (K_s)	-

A. Variation of Rotor Speed

This section will show the simulation results with different variation of speeds. The rotor will simulate at 18000 RPM, 14000 RPM and 10000 RPM. Figs. 6-8 illustrate the rotor orbit of both touchdown bearings (front and rear) with different speeds. From the results can be seen that every speed has different rotor orbit. The higher the speed, the bigger the orbit. Therefore, the biggest rotor orbit is occurred at the rotor speed of 18000 RPM. All the rotors will be dropped and the oscillation is occurred in the bottom of the touchdown bearing. And sometimes the jump motion also occurred as shown in Figs. 6 and 7, especially at the rear touchdown bearing.

Then, the displacements of the rotor can be seen from the rotor response as shown in Figs. 9-11. Based on the entire rotor responses are illustrated that the rotor will drop to the bottom of touchdown bearing and touch the inner race because the displacements exceed than the gap of touchdown bearing (1x10^{-4} m). Along with the increment of rotor speed, the rotor displacements become higher. When the rotor speed is 18000 RPM, the rotor displacement not only occurred in negative y-displacement but also in positive y-displacement. That condition also occurred at the speed of 14000 RPM, but the displacements are lower than 18000 RPM.

However, from all of the results can be indicated that the orbit and the rotor responses are less than critical clearance of 2x10^{-4} m. The maximum displacements are 1.0x10^{-4} m in x-displacements and 1.20x10^{-4} m in y-displacements for front touchdown bearing, while the maximum displacements of rear touchdown bearing are 1.10x10^{-4} m in x-displacement and 1.20x10^{-4} m in y-displacement.

When the rotor is dropped on touchdown bearings, there will be a contact between the rotor and inner race of touchdown bearings. Therefore, during the drop event, the system will generate the contact force as shown in Figs. 12-14. The magnitude of contact force is related to the rotor response. Therefore, the highest contact force is occurred when the rotor speed is 18000 RPM, the maximum forces of both touchdown bearings are 2.3x10^4 N for front touchdown bearing and 2.35x10^4 N for rear touchdown bearing. While maximum contact force at 15000 RPM for both touchdown bearings are 2.25x10^4 N and 2.15x10^4 N. Then the maximum contact force of front and rear touchdown bearing at rotor speed of 10000 RPM are 2.1x10^4 N and 1.9x10^4 N.

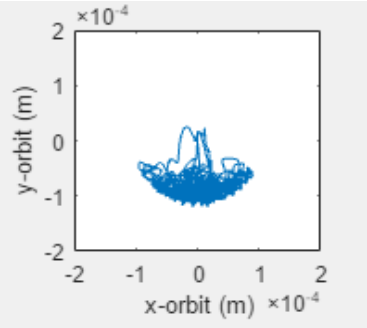

(a) Front touchdown bearing

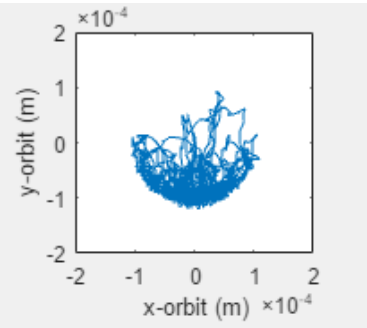

(b) Rear touchdown bearing

Figure 6. Rotor orbit at 18000 RPM

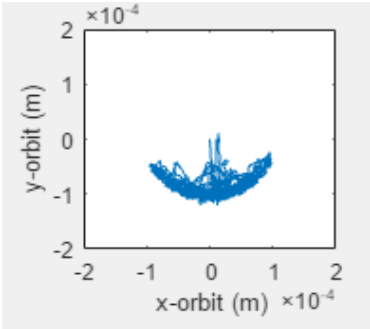

(a) Front touchdown bearing

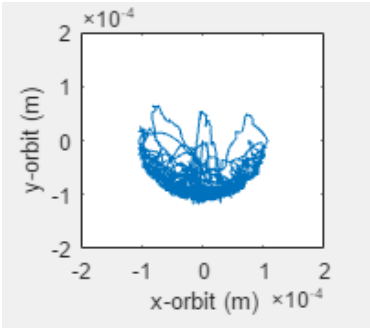

(b) Rear touchdown bearing

Figure 7. Rotor orbit at 14000 RPM

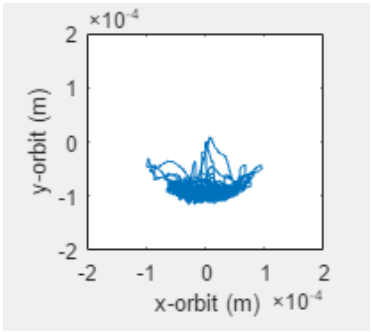

(a) Front touchdown bearing

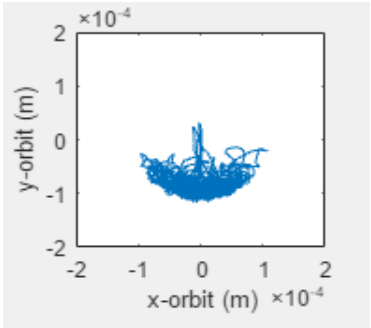

(b) Rear touchdown bearing

Figure 8. Rotor orbit at 10000 RPM

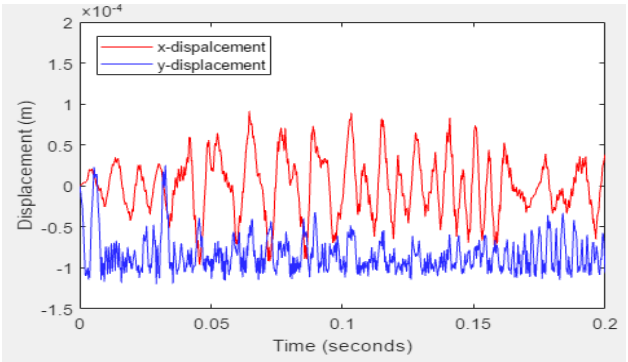

(a) Front touchdown bearing

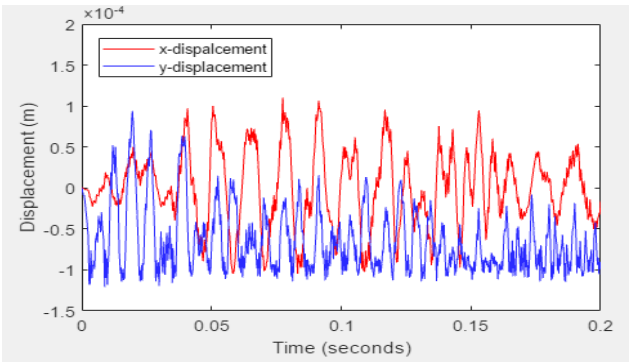

(b) Rear touchdown bearing

Figure 9. Rotor response at 18000 RPM

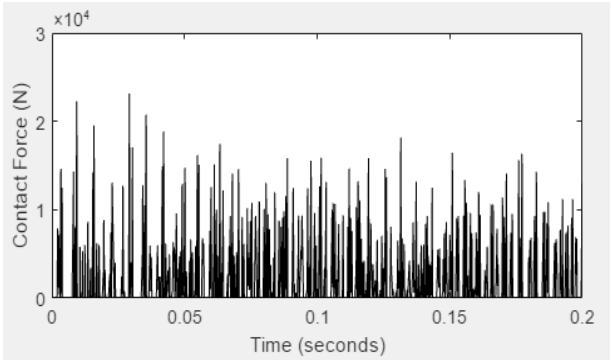

(a) Front touchdown bearing

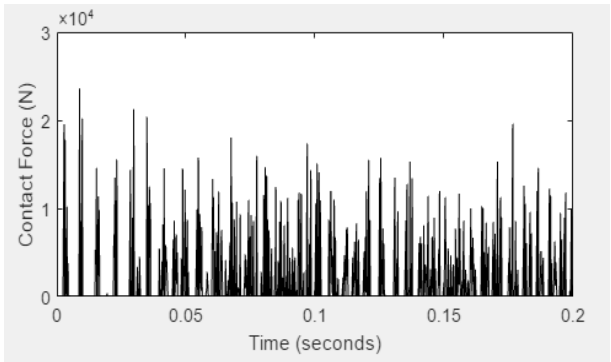

(b) Rear touchdown bearing

Figure 12. Contact force at 18000 RPM

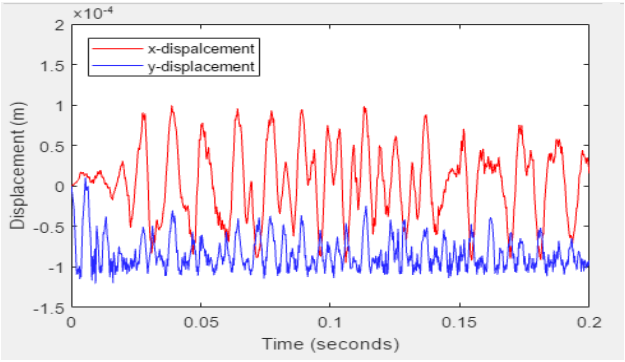

(a) Front touchdown bearing

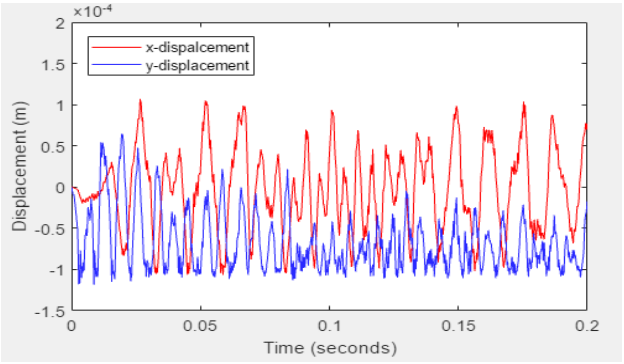

(b) Rear touchdown bearing

Figure 10. Rotor response at 14000 RPM

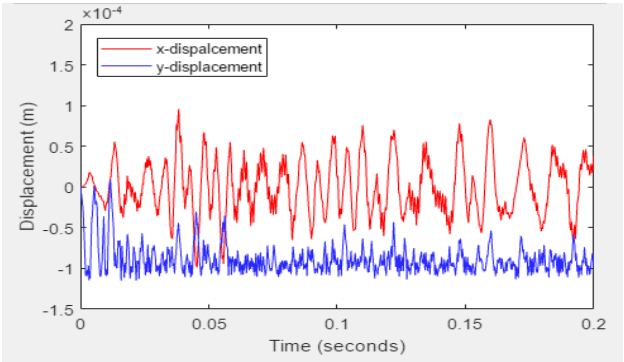

(a) Front touchdown bearing

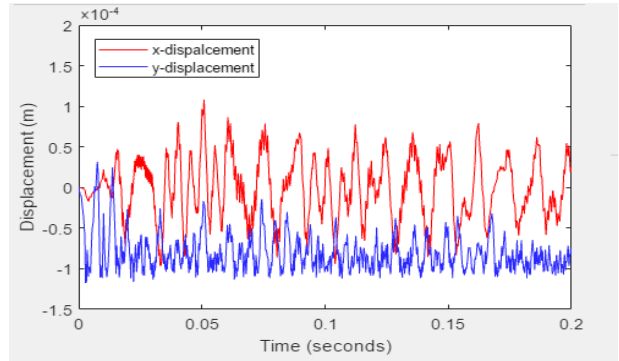

(b) Rear touchdown bearing

Figure 11. Rotor response at 10000 RPM

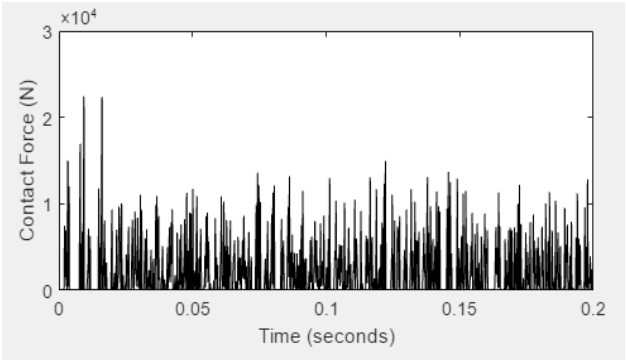

(a) Front touchdown bearing

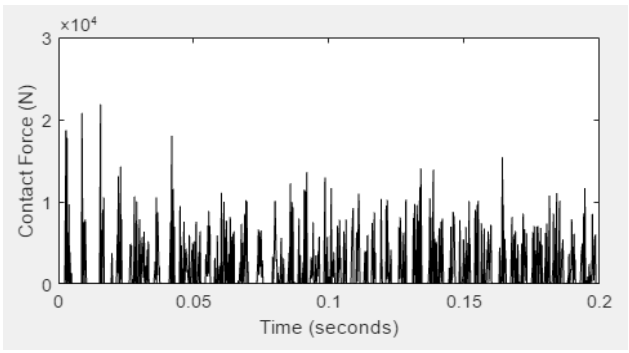

(b) Rear touchdown bearing

Figure 13. Contact force at 14000 RPM

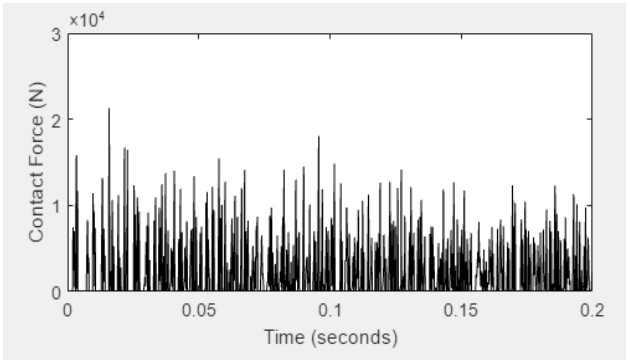

(a) Front touchdown bearing

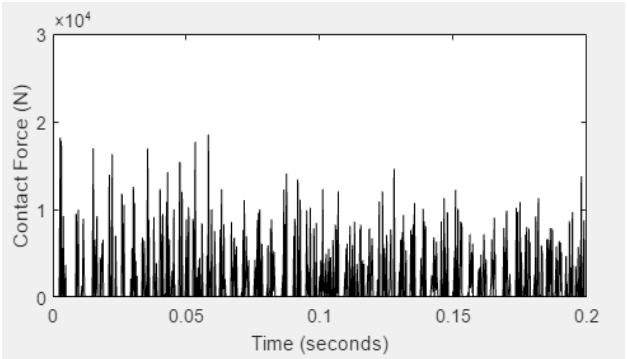

(b) Rear touchdown bearing

Figure 14. Contact force at 10000 RPM

Beside that when the rotor and touchdown bearings are in contact, the touchdown bearings speed will increase up to rotor speed, while the rotor speed will decelerate. The rotor deceleration and inner race deceleration are shown in Fig. 15 with the rotor speed is 18000 RPM (1885 rad/s). The inner race acceleration increase very fast due to the inner race moment of inertia is smaller than rotor moment of inertia.

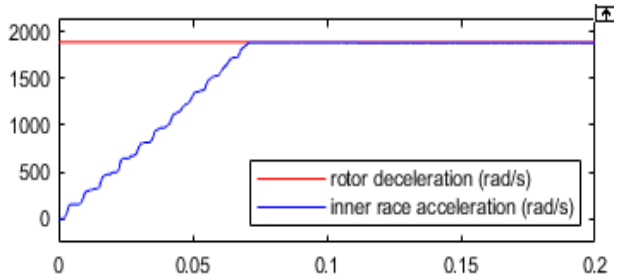

Figure 15. Rotor deceleration

B. *Effect of Damping Support and Stiffness Support*

The improvement to the original design is adding the support components such as damping support (C_s) and stiffness support(K_s). Fig. 16 illustrates the additional design of damping and stiffness support to the touchdown bearing original design. The value of damping and stiffness support are referring to Antti et.al [14], where C_s = 27900 Ns/m and K_s = 5x10^8 N/m.

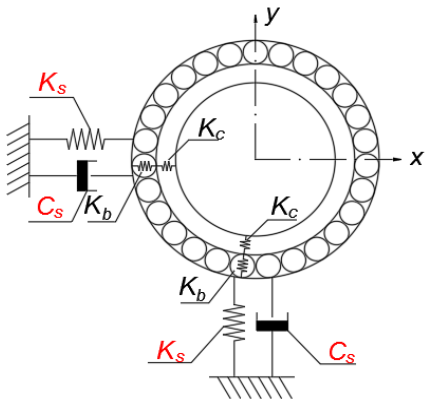

Figure 16. Ball bearing with damping support and stiffness support

Figs. 17-19 show the simulation results of both touchdown bearings (front and rear) with the addition of damping support and stiffness support at the case of 18000 RPM. The improvement brings the effect to the rotor behavior. As shown in Figs. 17 and 18, the orbit and the rotor displacement are smaller than before the improvement. All the x-displacements of both touchdown bearings are still in the gap, there is no contact between the rotor and inner race. And also for the y-displacements, if compared with the displacements as shown in Fig. 9, positive y-displacements in Fig. 17 are decrease after the addition of damping and stiffness support.

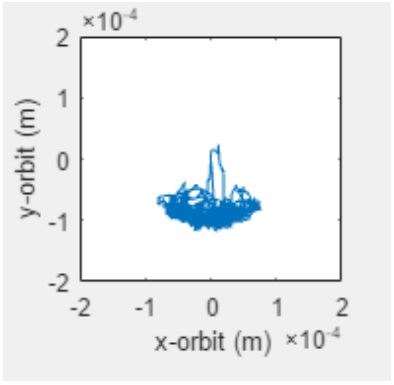

(a) Front touchdown bearing

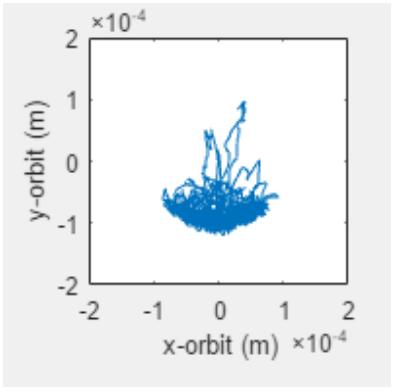

(b) Rear touchdown bearing

Figure 17. Rotor orbit at 18000 RPM with damping and stiffness support

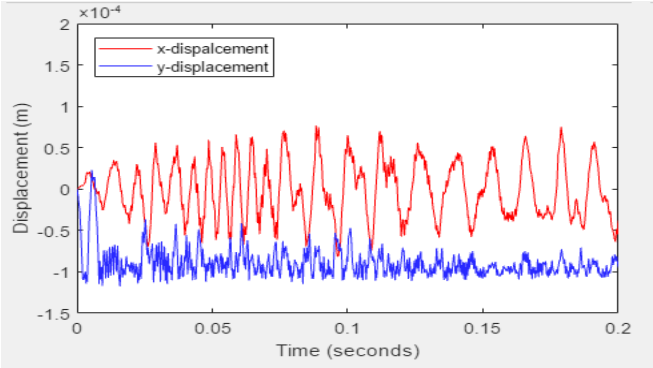

(a) Front touchdown bearing

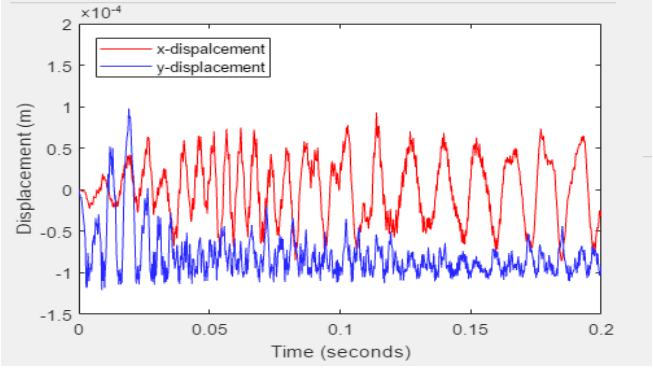

(b) Rear touchdown bearing

Figure 18. Rotor response at 18000 RPM with damping and stiffness support

The improvement of the original design also can be affected to the contact force as shown in Fig. 19. With the existence of supporting components (damping and stiffness support), the contact force can be reduced. The maximum contact forces are same; around 2.3x104 N, but after 0.1 sec contact forces decrease if compared with the contact force of original design in Fig. 12.

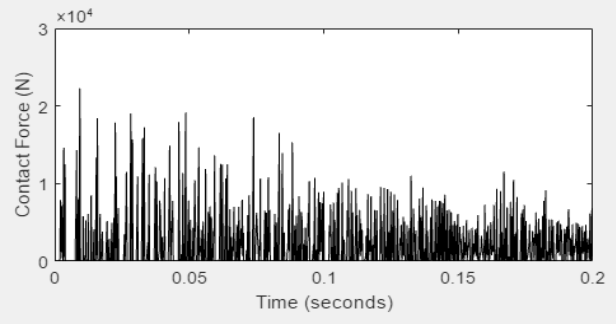

(a) Front touchdown bearing

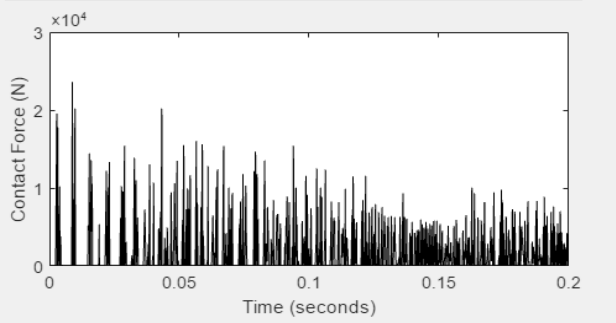

(b) Rear touchdown bearing

Figure 19. Contact force at 18000 RPM with damping and stiffness support

V. CONCLUSION

In this paper, the dynamic of the rotor system during power loss condition was investigated using Finite Element Method. Based on the results, the effect of rotor speed can be affected to the rotor behavior. On the other hand, the design of touchdown bearings also brings a very important role to the simulation results. Particularly, the addition of damping support and stiffness support can reduce the contact force between the rotor and the inner race touchdown bearing.

Therefore, conducting this dynamic simulation is very useful to analyze the rotor behavior. Moreover, from this study also can be used as an evaluation method to the original design so that the system can be improved in the future. Considering another improvement of the touchdown bearings design is necessary for further study.

ACKNOWLEDGEMENTS

The authors would like to thank the Bureau of Energy, Ministry of Economic Affairs, Taiwan, R.O.C., for supporting this research.

REFERENCES

[1] G. Sun, "Detailed ball bearing model for magnetic suspension auxiliary service," *Journal of Sound and Vibration*, vol. 269, pp. 933-963, 2004.

[2] J. Cao, T. Dimond, P. Allaire, and S. Dousti, "Auxiliary bearing system optimization for AMB supported rotor based on rotor drop analysis-Part I: rotor drop analysis method," *Proceedings on Int. Conf ASME Turbo Expo*, 2016.

[3] C.A. Fonseca, I.F. Santos, and H.I. Weber, "Influence ofunbalance levels on nonlinear dynamic of a rotor-backup rolling bearing system," *Journal of Sound and Vibration*, vol. 394, pp. 482-496, 2017.

[4] S. Zeng, "Modelling and experimental study of transient resopnse of an active magnetic bearing rotor during rotor drop on back-up bearings," *Proceedings of The Institution of Mechanical Engineers Part I, Int, Journal of Sound and Vibration*, vol. 394, pp. 482-496, 2003.

[5] G. Schweitzer, "Safety and reliability aspects for active magnetic bearing applications - A survey," *Proc. of the Institution of Mechanical Engineers Part I: Int. Journal of Systems and Control Engineering*, vol. 219, no. 6, pp. 383-392, 2005.

[6] J.C. Ji, C.H. Hansen, and A.C. Zander, "Nonlinear dynamics of magnetic bearing systems," *Int. Journal of Intelligent Material Systems and Structures*, vol. 19, no. 12, pp. 1471-1491, 2008.

[7] J.W. Zu and Z. Ji, "An improved transfer matrix method for steady-state analysis of nonlinear rotor-bearing systems," *Int. Journal pf Engineering for Gas Turbines and Power*, vol. 124, no. 2, pp.303-311, 2002.

[8] E.N. Cuesta, L.U. Medina, V.R. Rastelli, N.I. Montbrun, and S.E. Diaz "A simple kinematic model for the behaviour of a magnetically levitated rotor operating in overload regime," *Proceedings ASME Turbo Expo*, 2003.

[9] J.I. Inayat-Hussain, "Nonlinear dynamics of a magnetically supported rigid rotor in auxiliary bearing*," Int. Jornal of Mechanism and Machine Theory*, vol. 45, pp. 1651-1667, 2010.

[10] H. Ecker, "Nonlinear stability analysis of a single mass rotor contacting a rigid backup bearing," *Proceedings on Euromech Colloquium*, pp. 79-89, 1998.

[11] C. Liu, K. Zhang, and R. Yang, "The FEM analysis and approximate model for cylindrical joints with clearances," *Journal of Mechanism and Machine Theory*, vol. 42, pp. 183-197, 2007.

[12] Harris, T. A. and Kotzalas, M. N., "Rolling bearing analysis: essential concepts of bearing technology," 5th Ed., Taylor & Francis Group, New York, 2007.

[13] A. Karkkainen, J. Sopanen, and A. Mikkola, "Dynamic simulation of a flexible rotor during drop on retainer bearings," *Journal of Sound and Vibration*, vol.306, pp. 601-617, 2007.

[14] A. Karkkainen, J. Sopanen, and A. Mikkola, "Simulation of AMB supported rotor during drop on retainer bearing," Research Report. Lappeenranta University of Technology, April.